



# Eutrophication hotspots, nitrogen fluxes and climate impacts in estuarine ecosystems: A model study of the Odra estuary system

Johannes Pein<sup>1</sup> · Joanna Staneva<sup>1</sup>

Received: 26 September 2023 / Accepted: 19 February 2024 / Published online: 5 March 2024  
© The Author(s) 2024

## Abstract

The Odra estuary in the southern Baltic Sea comprises the Odra (Szczecin) Lagoon, the Pomeranian Bay and a number of other shallow water areas and channels. Known for its abundance of fish, eutrophication in the Odra Lagoon is a pressing issue for science and environmental management representing a global problem: What determines the seasonal variability of nitrogen and nitrogen turnover in shallow water areas, and how does seasonal variability change due to climatic changes such as warming and sea level rise? How do such changes affect nutrient exports to the regional ocean? This study employs a high-resolution unstructured model system to investigate physical-biogeochemical interactions, nitrogen turnover, and conditions leading to nitrogen export to the Baltic Sea within the Odra estuary. The research comprises hindcast and a climatic experiment with modified water level and temperature inputs. The model reproduces the thermohaline dynamics of brackish shallow water areas, phytoplankton blooms and the variability of inorganic nitrogen. The simulations identify the dynamic partitioning of the Odra Lagoon into the highly eutrophic, lake-like Small Lagoon and more frequently flushed, zooplankton-rich Great Lagoon. Although the two years of the hindcast simulation feature very different boundary conditions in terms of river forcing, comparable patterns of seasonal nitrogen export emerge. In a climate change experiment with increased sea levels and global temperatures, the system appears sensitive, but remains stable with regard to nutrient transport and is therefore predictable. The climate change experiment reveals enhanced primary producer biomass concentrations, suggesting heightened eutrophication. While in the shallow waters of Odra Lagoon oxygen concentration remains relatively stable, oxygen depletion intensifies as the lagoon outflows enter the Pomeranian Bay. This phenomenon is linked to increased denitrification within the stratified Odra plume. Deeper, meandering channels, such as Swina, demonstrate resilience to oxygen reduction, influenced by sea level rise and enhanced currents. Based on the temporal-spatial high-resolution coupled, validated simulations, it is possible to develop tailor-made management solutions without having to run expensive and complicated observation campaigns in the shallow waters with complex topography.

**Keywords** Eutrophication · Nitrogen cycling · Seasonal nitrogen fluxes · Estuarine ecosystems · Ecological model · Coupled ocean- biogeochemical model · Odra estuary

---

This article is part of a Topical Collection on the *13th International Workshop on Modeling the Ocean (IWMO), Hamburg, Germany, 27-30 June 2023*.

---

Responsible Editor: J. Staneva, J. Wang, O. Fringer and R. Camargo

---

✉ Johannes Pein  
johannes.pein@hereon.de

<sup>1</sup> Helmholtz-Zentrum Hereon, Max-Planck-Str. 1,  
21502 Geesthacht, Germany

## 1 Introduction

Lagoons and estuaries belong to the land-ocean transition zone that is characterized by high physical-biogeochemical gradients and complex interactions. This dynamic region is marked by dramatic shifts in both physical and biogeochemical properties, fostering intricate and multifaceted interactions. While water bodies with relatively large depths and high flow velocities are classified as estuaries, lagoons are considered as distinct shallow water landscapes with low flow velocities and high importance of the sediment layer for biogeochemical turnover (Kjerfve 1986; Deborde et al. 2008). This key systemic feature leads to the lagoon taking

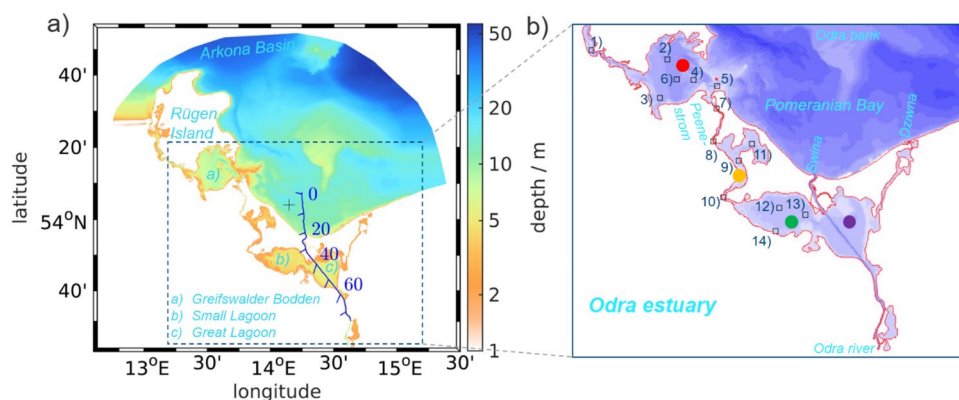


**Fig. 1** **a** Model area where the background color indicates depth. The blue solid line represents a transect that is used for dynamical analysis in the manuscript. The black cross marks the position of shipborne profile measurements. In **b** the indices and positions of permanent observation stations in the area of the Odra estuary are shown

(for stations names see Supplementary Table 1). The colored circles identify the following subregions: red – Greifswalder Bodden, yellow – Peenestrom, green – Small Lagoon, purple – Great Lagoon

up, storing and releasing nutrients such as nitrogen to drive internal primary production. Lagoons and estuaries are inherently predisposed to be eutrophic systems due to their intrinsic biogeochemical processes and nutrient cycling patterns (Voss et al. 2021; Schernewski et al. 2023). Despite the best efforts to regulate and curtail nutrient inputs into these systems, their natural eutrophic tendencies persist, and they cannot be effortlessly transformed into non-eutrophic waters. Given the intricate interplay of complex factors that maintain the behavior and ecological significance of lagoons, a comprehensive understanding of their internal dynamics is crucial. Understanding these factors is pivotal in devising management strategies that adeptly navigate the intricate temporal and spatial dynamics of these ecosystems. The successful management and preservation of lagoons demand a profound recognition of their inherent attributes, their pivotal role as nutrient reservoirs, and their profound significance as ever-evolving ecosystems seamlessly integrated within the land-ocean transition zone.

The Odra estuary in the Baltic Sea is a borderline case between estuary and lagoon (for geographical information see Fig. 1a; Chojnacki 1999; Osadczuk et al. 2007). While the Baltic Sea itself is considered a large estuary, the extensive shallow water zone at the lower reaches of the Odra river, which are shielded from the Baltic Sea by narrow barrier islands, is called Odra or Szczecin Lagoon. Piercing through the barrier islands, three channels route freshwater towards the Baltic Sea proper, the largest of which – Swina – represents the main route of Odra river discharge to the ocean (Mohrholz and Lass 1998; Radziejewska and Schernewski 2008). The extension of Swina towards the port of Szczecin has been developed to function as a navigational channel, with a minimum depth of 12 m. In contrast, the other channels—Peene and Dziwna—often have depths not exceeding 2 m. Stretching nearly 50 km from west to east,

the Odra Lagoon’s coastline is extending over 150 km. The lagoon is zonally divided by land spits, creating a separation between the shallower western Small Lagoon and the deeper eastern Great Lagoon, which also serves as the passage for the shipping channel to Swina (Fig. 1b).

The water budget of Szczecin lagoon is dominated by river discharge and intrusion of Baltic Sea water that contribute some  $15 \text{ km}^3 \text{ yr}^{-1}$  and  $7.5 \text{ km}^3 \text{ yr}^{-1}$ , respectively (Chojnacki 1999). Apart from routing freshwater, the lagoon outlets are also gateways of inflow of pulses of brackish water from Baltic Sea into the lagoon (Mohrholz and Lass 1998; Radziejewska and Schernewski 2008). This way, lagoon dynamics couple with dynamics in the Pomeranian Bay where flows are controlled by various factors such as saline inflows from North Sea, buoyancy forcing from Odra and tributaries and the coastal geometry (Kowalewska et al. 2003). The internal dynamics can also be complex, for example, water from the Odra river can intrude the Small Lagoon perturbing its stable eddies. During storm surges, the water masses entering the Swina Channel block the downstream freshwater flow, which leads to extreme flood risk in case of additional river floods (Kowalewska-Kalkowska 2021). For centuries, the lagoon has been exploited for its natural abundance, with fishing regulated as early as the sixteenth century (Schernewski et al. 2023). Contemporary science agrees that the Odra Lagoon has exceptionally high primary and secondary production (Stokowski et al. 2020), although the observational basis is sparse as only few measurements of actual production rates have been performed (Kowalewska et al. 2003; Radziejewska and Schernewski 2008). There is also agreement that primary production in lagoons is light-limited, although frequent nitrogen depletion in recent years indicates that nutrient limitation cannot be ruled out, especially as background nutrient inputs have been declining for decades (Schernewski et al. 2023). Primary

production is also potentially relevant for the transport of pollutants. Plankton-borne organics adsorb organic pollutants whereas the strength of the bonds depends on ambient oxygen conditions, availability of sediments and hydrologic conditions (Kowalewska et al. 2003).

It is known that the Odra Lagoon acts as a buffer for nutrient and organic loads and mitigates the eutrophication of the Baltic Sea proper. Recently, it has been described as a naturally eutrophying system (Chojnacki 1999; Schernewski et al. 2023). Internal nutrient cycling is thought to fuel the primary production of the lagoon. The actual buffer is a fluffy sediment layer, containing a high proportion of organic matter derived from phyto-detritus (Radziejewska and Schernewski 2008; Schiewer and Gerald 2004). The degree of eutrophication of the Odra Lagoon is high, as evidenced by small Secchi depths and temporal occurrence of hypoxia (Friedland et al. 2019; Radziejewska and Schernewski 2008; Schernewski et al. 2011). One reason for the high turbidity is the extremely high annual primary production, which in the area of the Great Lagoon, for example, reportedly may reach a multiple of the average primary production of estuaries worldwide (Stokowski et al. 2020). The oxygen deficiency phenomena drive release of phosphorus from sediments and are suspected to increase fish mortality (Radziejewska and Schernewski 2008; Schernewski et al. 2011). The Baltic Marine Environment Protection Commission (HELCOM<sup>1</sup>) recommended the development of a eutrophication management programme at the beginning of the century (Radziejewska and Schernewski 2008). In recent years, research into the exact eutrophication status according to the Water Framework Directive and its appropriate individual interpretation in relation to the Odra Lagoon continues (Friedland et al. 2019). Proposed strategies to improve the environmental status of the Odra Lagoon include mussel cultivation and restoration of macrophytes (Schernewski et al. 2012, 2023). Besides problematic the long-term conditions, extreme events such as river floods can mobilise deposited organic material, which carries large amounts of nutrients and pollutants and drives oxygen depletion (Siegel et al. 1998; Kowalewska et al. 2003). In recent years, dramatic fish kills have repeatedly occurred in the Odra river. In the public discussion, hypoxia and toxic algal blooms are mentioned as possible causes. These developments are probably caused by increasing water temperatures and increasing salinity against the background of sea level rise and could be seen as harbingers of the consequences of climate change.

The high primary production and related biochemical turnover make the Odra Lagoon vulnerable to extreme hydrodynamic, meteorological and biogeochemical conditions. Precise knowledge of the circumstances and processes

leading to the formation of so-called hotspots is incomplete, but is urgently needed so that management to maintain ecosystem functions can be precisely addressed. Previous studies have shown that the reduction of nutrient inputs has somewhat reduced the pressure on the Odra Lagoon but that seasonal nutrient variability and exports to the Baltic Sea have not yet been properly elucidated (Friedland et al. 2019; Schernewski et al. 2023). Furthermore, projected sea level rise and temperature increase indicate continued increased environmental pressure on coastal ecosystems such as the Odra estuary. Higher-end scenarios such as RCP8.5 project median sea level rise of more than 0.7 m and summer surface temperature rise by at least 2.5 °C in the area of the southern Baltic Sea at the end of the century (see Table 2 in Grinstead et al. 2015; Fig. S6 in Meier et al. 2019). Although tides play almost no role here, a higher sea level could nevertheless lead to altered stratification, currents and tracer transport. Warming almost always leads to increased oxygen depletion due to higher process rates, which in the absence of tides cannot be efficiently compensated by higher mixing of oxygen from the surface. This leads to the question what will be the response of a shallow water ecosystem like the Odra estuary to climate impacts? Will hypoxia spread from the deeper regions of the Baltic Sea to the shallow water areas? Will eutrophic exports increase? To answer these questions, we complement the hindcast runs with a simple climate experiment.

To better understand the genesis of hotspots of biogeochemical turnover in the Odra estuary system, we have developed a state-of-the-art coupled physical-ecological model that accounts for the main energy and matter fluxes into and out of our study area. The aims of this study are 1) to validate and demonstrate the predictive capacity of the model, 2) to quantify the physical controls on seasonal nutrient cycling, 3) to assess the potential impacts of climate change, and 4) to quantify nutrient exports to the Baltic Sea under historic conditions and conditions of climatic change. To address climatic change, we complement the hindcast simulations with a simple climate experiment that accounts for sea level rise and global warming.

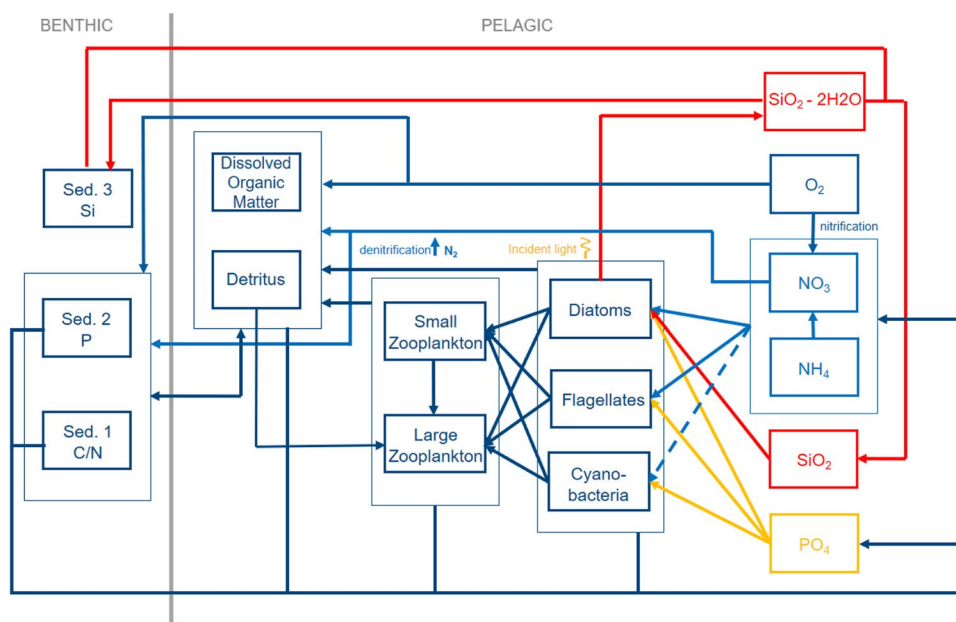
## 2 Methods

### 2.1 Model framework

In this study we use the Semi-implicit Cross-scale Hydroscience Integrated System Model (SCHISM; Zhang et al. 2016). It solves the Reynolds-averaged Navier-Stokes equations on unstructured grids. Thanks to the semi-implicit approach model integration is stable and relatively fast allowing a combination of coarse and high resolution regions in a single mesh. SCHISM has been successfully

<sup>1</sup> <https://helcom.fi/about-us/>

**Fig. 2** Scheme of the biogeochemical model ECOSMO II (adopted from Benkort et al. 2020). The biogeochemical parametrisations are given in Supplementary Table 2



applied to tackle the hydrodynamics of estuaries around the world such as Chesapeake Bay, San Francisco Bay, Ems estuary and many others (Ye et al. 2018; Wang et al. 2020; Pein et al. 2014; 2021a, b). Stanev et al. 2019 and Haid et al., 2020 have demonstrated that SCHISM is capable of simulating dynamics typical of the Baltic Sea such as summer stratification, major Baltic inflow events and the secondary circulation in the Danish straits. Given these experiences, the modelling framework is a promising candidate to simulate the three-dimensional flows in the Odra (Szczecin) Lagoon and Pomeranian Bay.

Here we use SCHISM in combination with an ecological model of the lower trophic levels, ECOSMO II (Schrum et al. 2006; Daewel and Schrum 2013; Yumruktepe et al. 2022). The modelling framework SCHISM-FABM-ECOSMO has recently been applied to examine the nutrient turnover in the tidal and heavily eutrophied Elbe estuary (Pein et al. 2021a, b), whereas FABM refers to the coupling interface between the hydrodynamic and the ecology parts of the code (Bruggeman and Bolding 2014). The coupled model takes into account barotropic and baroclinic currents, water level, turbulent mixing and tracer transport. Transport of biogeochemical tracers by the physical model occurs at every model time step. The ecological module ECOSMO takes into account 1) inorganic nutrients such as nitrate, ammonium, silicate and phosphate; 2) three functional groups of primary producers – namely small phytoplankton, diatoms and cyanobacteria, 3) two functional groups of secondary producers – namely small and meso-zooplankton, 4) dissolved oxygen, 5) particulate organic nitrogen (phytodetritus) and opal (particulate silicate) and 6) dissolved inorganic carbon (see schematic in Fig. 2). ECOSMO II sticks to

the Redfield ratio. In addition to the pelagic biogeochemical kinetics, the model allows for storage of particulate nutrient pools of C + N, Si and P in a sedimentary layer. The particulate nutrients can be eroded from the sedimentary when the critical shear stress is exceeded. In the deposited state, the bottom nutrients are subject to mineralization or further transformation such as denitrification in case of bottom nitrogen. Part of the bottom nutrients is buried according to a constant rate leaving the system. Denitrification occurs at low oxygen conditions and leads to irretrievable loss of inorganic nitrogen via outgassing. For further details, see Daewel and Schrum (2013) and Pein et al. (2021a).

In the configuration used here, the model code was slightly extended compared to Pein et al. (2021a, b). We have enabled the simulation of inorganic sediment dynamics in SCHISM (Pinto et al. 2012; Stanev et al. 2019) using the sediment fractions representative of light sand and silt. The sand and silt distribution was initialized following literature and online resources (Osadczyk and Wawrzyniak-Wydrowska 1998; Baltic Sea portal of IOW at <http://bio-50.io-warne-muende.de/iowbsa> (last accessed 5 September 2023)). Suspended sediment concentrations are passed to ECOSMO, where they contribute to light attenuation through phyto-detritus and phytoplankton self-shading. This leads to the following prescription of photosynthetically active radiation

$$I(x, y, z, t) = \frac{I_s(x, y)}{2} \exp \left( -k_w z - k_{tss} - k_{phyto} \int_z^0 \sum_{j=1}^3 C_{Pj} \partial z \right), \quad (1)$$

where  $I_s$  is short wave radiation,  $k_w$  is water extinction coefficient,  $k_{tss}$  is total suspended sediment extinction coefficient,

$k_{phyto}$  is phytoplankton extinction coefficient,  $C_{pj}$  is the local biomass concentration of the functional phytoplankton species with index  $j$ , and  $x, y, z$  are meridional, zonal and vertical coordinates, respectively (adopted from Daewel and Schrum 2013).

## 2.2 Forcing

The model forcing consists of an oceanic part, a terrestrial part and the meteorological forcing. The meteorological forcing includes wind fields, surface temperature, incoming short wave and long wave radiation and precipitation from the reanalysis of the German weather service (see Kaspar et al. 2020). All meteorological data have hourly time resolution and spatial resolution is  $7 \times 7$  km. In order to drive water level, currents, salinity and temperature at the open boundary, we use the reanalysis of daily physics from the Danish Meteorological Institute's Baltic Sea model provided via the Copernicus service (Product ID: "BALTICSEA\_MULTI-YEAR\_PHY\_003\_011", last access 21 June 2019, <sup>2</sup> <https://doi.org/10.48670/moi-00013>). The model has horizontal resolution of  $2 \times 2$  km and up to 56 vertical levels. All forcing variables are prescribed directly at the open boundary using clamped boundary conditions. Salinity and temperature are additionally prescribed within a sponge layer of 10 km along the open boundary. The same treatment applies to dissolved nutrients, oxygen and plankton which have been sampled from a hind-cast North Sea and Baltic Sea simulation of the stand-alone ECOSMO model (Daewel and Schrum 2017a, b). Both simulations, the physical reanalysis and the biogeochemical hind-cast simulations represent the same period of 2012 and 2013.

At the land side, the Odra, Peene and Zarow/Ücker rivers discharge water volume and nutrient loads into the model area. Daily Odra discharge has been downloaded from the Global Runoff Data Base.<sup>3</sup> River run-off from the small tributaries is based on monthly climatology from the Deutsches Gewässerkundliches Jahrbuch.<sup>4</sup> The nutrient concentrations of nitrate, silicate and phosphate of the small tributaries stem from observations kindly provided by the State office for environment, environmental protection and geology Mecklenburg-Vorpommern (LUNG).<sup>5</sup> The nutrient concentrations of Odra river water have been compiled from different sources, namely the Polish-German project "International commission for the protection of the

Odra against pollution",<sup>6</sup> estimates of SMHI ehype model simulations<sup>7</sup> and literature data.

## 2.3 Observations

The environmental agency of the federal state of Mecklenburg-Vorpommern (Landesamt für Umwelt, Naturschutz und Geologie (LUNG)) operates more than fifty permanent measuring stations along the German Baltic coast. For the purpose of mode-data comparison we use a subset of 14 stations that are located in the inner waters of the Odra estuary (see indexing and geographical information Supplementary Table 1, Fig. 1b; LUNG 2016). All stations collect monthly temperature, salinity, nutrient and oxygen concentrations at the water surface. During the productive seasons chlorophyll-a is also sampled.

## 2.4 Specific methodology

In the following we shortly expose the specific methods used to tackle the research questions formulated at the end of the introductory section. The specific methodology for answering the research questions uses as a basis the numerical modelling and observations introduced in the previous subsections.

### 2.4.1 Model calibration and validation

During the calibration of the model, measurements of salinity, temperature, chlorophyll and inorganic nitrogen are selected from the period covered by the forcing data. These variables are then sampled from the model output fields and compared to respective time series from model test runs. The model test runs typically cover one year. While iterating the model, critical parameters such as bottom drag and light attenuation coefficients parameters are successively adjusted to minimize the difference between simulated and observed variables (not shown). For model validation, these comparisons are repeated for all available measurement stations and the entire simulation period. For the graphical diagnosis of the quantitative agreement between model and observations in the study area, we use a Taylor diagram (Taylor 2001). This measure assesses the quality of the model simulation with respect to target variables by spanning a space defined by the normalised standard deviation, the normalised rmse and the correlation coefficient  $R$ . We use the Taylor diagram to evaluate model performance with respect to surface salinity, water temperature, chlorophyll concentration and inorganic nitrogen concentration. In this diagram, a perfect

<sup>2</sup> [https://data.marine.copernicus.eu/product/BALTICSEA\\_MULTI-YEAR\\_PHY\\_003\\_011/description](https://data.marine.copernicus.eu/product/BALTICSEA_MULTI-YEAR_PHY_003_011/description)

<sup>3</sup> [https://www.bafg.de/GRDC/EN/01\\_GRDC/13\\_dtbse/database\\_node.html](https://www.bafg.de/GRDC/EN/01_GRDC/13_dtbse/database_node.html)

<sup>4</sup> <https://www.dgj.de/>

<sup>5</sup> <https://www.lung.mv-regierung.de/>

<sup>6</sup> <https://www.mkoo.pl/index.php?mid=35&lang=DE>

<sup>7</sup> <https://hypeweb.smhi.se/>

model simulation is indicated by a marker at the intersection of the x-axis and the circle with a radius of one standard deviation. Shifting of the markers towards the regions with increased mean square error and decreased correlation coefficient indicate deviations of the model simulation from the observed reality.

#### 2.4.2 Physical controls

Hydrodynamic processes in the investigated water body can strongly influence the biogeochemical turnover and variables such as the oxygen content and the remineralisation of ammonium. In coastal waters such as estuaries and lagoons, the residence time and stratification of the water column are particularly relevant. Both determine how intensively and for how long the water volume in an area is isolated from external inputs or exchange, whereby these purely physical processes can anticipate the effects of biogeochemical turnover such as oxygen depletion or accumulation of nitrogen. As the residence time cannot be calculated directly by the model, we use water age here to represent the quality of water exchange between an area and surrounding areas. During the model simulation, an age tracer is defined for each open boundary such as river and sea boundaries. This tracer enters the model area at each model time step being assigned age zero. During advection in the model domain, the age of the tracer in the reference volume increases with time, while it simultaneously adapts through exchange with adjacent water masses of younger or older age. The details of this method are given in Shen and Haas (2004).

A suitable measure for estimating the stratification is the potential energy anomaly (Simpson 1981):

$$\Phi = \frac{1}{D} \int_{-H}^{\eta} gz(\rho - \bar{\rho}) dz, \quad (2)$$

where  $\eta$  is the local water elevation and  $D = H + \eta$ .  $\Phi$  is about zero in well-mixed environments whereas  $\Phi > 1$  indicates stable stratification.

To substantiate the hypothesis of functional relationship between potential physical controls and biogeochemical key variables and processes we use Pearson's linear correlation coefficient ("R").

#### 2.4.3 Climatic change experiment

In order to answer the question of how the system under investigation potentially reacts to climatic changes, we conduct a simplified climatic experiment. For this purpose, the forcing fields of the validated hindcast are modified by changes to climatic variables such as sea level and temperature. To test the sensitivity of the Odra estuary system to climatic change, the hind-cast experiment has been repeated

with increased sea level and temperature. Sea level rise of 1 m has been mimicked by increasing the bathymetric depth by 1 m globally. To enhance water temperatures globally, temperatures at the open boundaries were increased by 4 °C at the open boundary, river boundaries and for air temperature at the sea surface. These applied changes approximate changes to Baltic sea level and water/air temperature under the RCP8.5 scenario at the end of the century (Grinsted et al. 2015; Meier et al. 2019). Note that "ref" refers to reference simulation and "scen" refers to climatic change scenario throughout the paper.

#### 2.4.4 Nitrogen fluxes

To determine the nitrogen transports from the outlets of the Odra Lagoon into the Baltic Sea, the SCHISM option is used to calculate fluxes of water volume and solutes contained therein at the time step level. For this purpose, for each outlet we define a cross-transect separating the lagoon from the regional ocean. During model integration, the instantaneous nitrogen flux of a nitrogen species  $F_N(t)$  at a cross-section is calculated according to

$$F_N(t) = \sum_{j=1}^{n_j} \sum_{k=1}^{n_k} U(j, k, t) N(j, k, t) A(j, k, t), \quad (3)$$

where  $U$  is the orthogonal to the transect velocity,  $N$  is nitrogen and  $A$  is the area of the computational cell. Indices represent time ( $t$ ), cell along the cross-section ( $j$  with total number of cells  $n_j$ ) and vertical layer ( $k$  with total number of cells  $n_k$ ). The model saves the sum of fluxes of the nitrogen species across a section during each model time step. To derive the time-averaged fluxes during a month or a year, the instantaneous fluxes are averaged over the respective period during post-processing (see also Hosseini et al. 2023).

## 3 Results

The model has been integrated for the period of 1 January 2012 to 31 December 2013. Model spin-up was one year (2012) to assure realistic initial distribution of thermo-haline fields and pools of inorganic nutrients in the surface sedimentary layer. In the following, we present the major physical and biogeochemical characteristics representative of the model simulations and supported by station observations.

### 3.1 Hydrodynamics of the Pomeranian Bay and Szczecin Lagoon

The ocean model simulations were validated using available observations of surface temperature and salinity in the Greifswalder Bodden, Peenestrom and Small Lagoon water bodies. Water temperature in shallow embayments

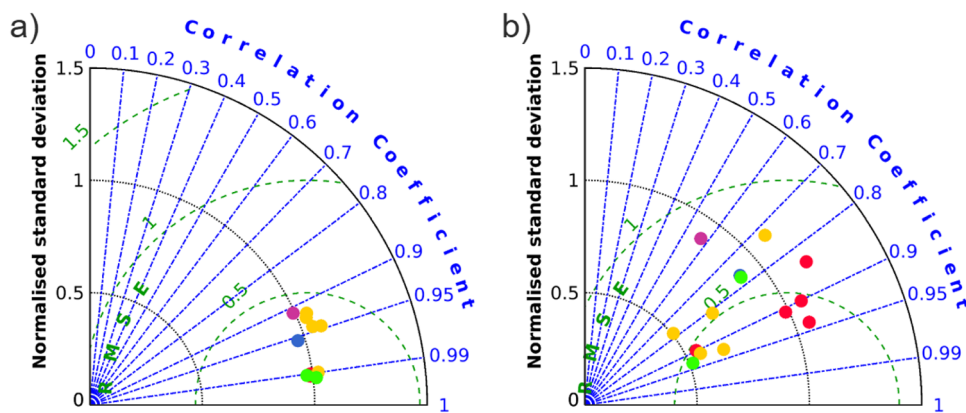
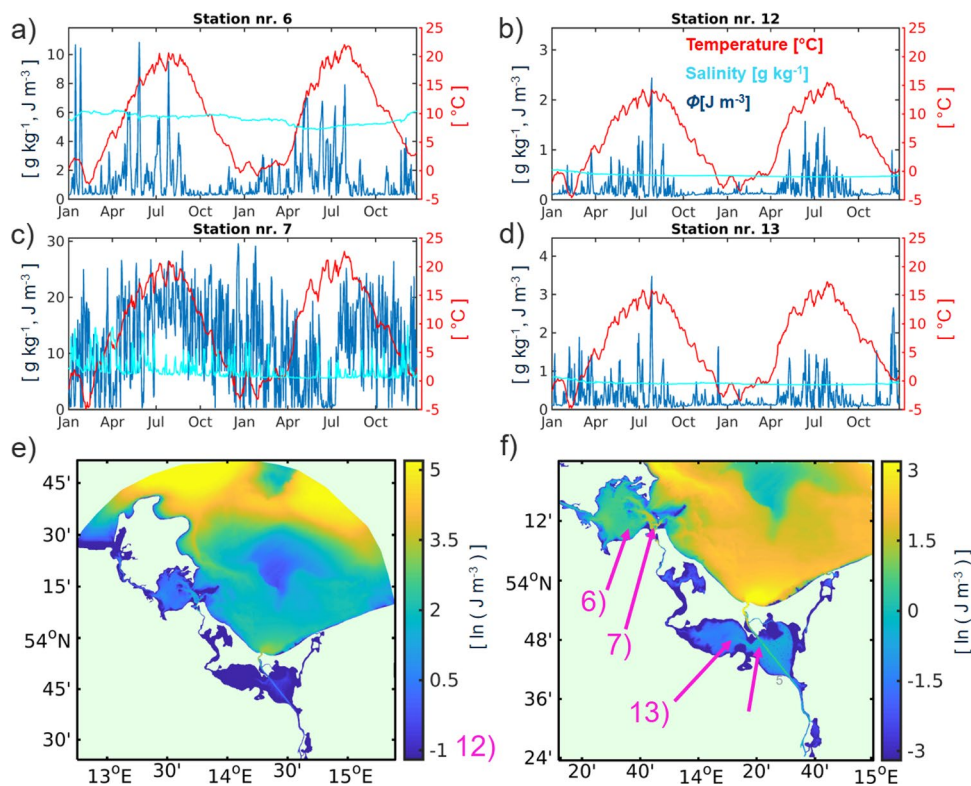


**Fig. 3** Taylor diagrams of **a** surface temperature and **b** surface salinity illustrate the agreement of model simulation with observation stations (see Fig. 1b) during 2012–2013. In these diagrams, each dot represents the mode-data comparison at a specific observation station. Red dots refer to stations of the Greifswalder Bodden, yellow dots to

the ones of Peenestrom and green dots represent stations in the area of the Small Lagoon. The blue dot refers to the Achterwasser station and the purple one represents the station Staatsgrenze (KHM, see Supplementary table S1)

**Fig. 4** **a–d** show time evolution of surface temperature, salinity and potential energy anomaly at four permanent observation stations (for legend see **b**, for location see **f**) and Fig. 1b). **e** Average potential energy anomaly  $\Phi$  and **f**  $\log(\Phi)$  during 2012–2013



is primarily a function of atmospheric influence. A Taylor diagram illustrates the agreement between simulated and observed water temperatures (Fig. 3a, station locations see Fig. 1b). The simulated temperature demonstrates a very high correlation with the observed time series and small errors. The dots cluster along the line representative of the ratio of observed to simulated standard deviations indicating consistent seasonal amplitudes of model and observations. A typical distribution of sea surface temperature is given in

Supplementary Figure S1a, which shows the average sea surface temperature between May – September 2012. A Taylor diagram of observed vs. simulated surface salinity reveals a larger scatter (Fig. 3b). The model simulations show high correlations and small errors with respect to observations in the Greifswalder Bodden. At most stations in the Peenestrom and at both Small Lagoon stations the model underestimates the amplitude of salinity fluctuations, whereas associations are higher than 0.7 still indicating high correlation.

Time series of simulated surface temperature and salinity at a couple of stations illustrate the dynamical similarities and differences of the different sub-regions of the Odra estuary. The station located in the center of the Greifswalder Bodden (station Nr. 6) manifests salinities around  $6 \text{ g kg}^{-1}$  without apparent small-scale fluctuations (Fig. 4a). The nearby station Nr. 7 at the entrance to the Peenestrom channel shows salinities of at least  $7 \text{ g kg}^{-1}$  with frequent pulses that reach as high as  $14 \text{ g kg}^{-1}$  (Fig. 4c) These salinity pulses are indicative of inflows of brackish Baltic Sea water towards the Small Lagoon (Lass et al. 2001). A typical salinity distribution is given in Supplementary figure S1b. The seasonal salinity variability is higher at the Peenestrom station confirming its intermittently changing exposure to predominantly marine or continental influence. Two stations in the Small Lagoon show small salinity concentrations below  $1 \text{ g kg}^{-1}$  but also smaller seasonal temperature variability (Fig. 4b, d). These stations reveal the dominance of freshwater influence in the Small Lagoon but also demonstrate resistance to excessive summer heating of central lagoon and Swina channel waters.

Eutrophied systems like the Odra estuary may suffer from stratification that reduces the vertical mixing of well-oxygenated surface water to the bottom. Due to the absence of significant tidal variability and the narrowness of the three outlets connecting the lagoon with the Baltic proper (Mohrholz and Lass 1998), frequent summer stratification over the deeper parts ( $h > 10 \text{ m}$ ) of the Odra estuary should not be surprising. To diagnose stratification we plot the potential energy anomaly (see sub-Sect. 2.4). According to this measure, the water column is mostly well-mixed at the Small Lagoon stations (Fig. 4b, d) with intermittent stratification during the summer months. Given the small salinity variability, the stratification events are apparently linked to surface heating. At station Nr. 7,  $\Phi$  is a multiple times higher with mixing happening only occasionally during winter (Fig. 4c). Here the pulses of high stratification correlate with the pulses of inflowing brackish water. In the center of Greifswalder Bodden (station Nr. 6) background stratification is weak but at times of rapid surface heating  $\Phi$  reaches maxima of up to  $10 \text{ J m}^{-3}$ . A map of average  $\Phi$  during the period of May to September of 2012 shows persistent stratification in the Baltic proper with weaker stratification in the area of the Pomeranian Bay (Fig. 4e). The shallow waters of the Small Lagoon and the Greifswalder Bodden demonstrate average mixed conditions. A zoomed-in view of the Odra estuary region showing  $\log \Phi$  reveals further details of the spatial variability of summer stratification (Fig. 4f). The outflow region of the Swina channel clearly emerges from the surrounding coastal waters of the Pomeranian Bay. The shallow Odra bank north of Pomeranian Bay is characterised by particularly low  $\Phi$  while the deep channel in front of Rügen islands manifests enhanced stratification similar to

the Swina outflow delta. Although the latter has a shallower bathymetric depth, both areas demonstrate similar dynamical depths. The Odra shipping channel inside the lagoon is identified by enhanced stratification, potentially affecting on the nutrient turnover in the lagoon and the export of nutrients to the Baltic Sea proper.

The current velocity fields in the outer Odra estuary are a function of the barotropic circulation in the Baltic proper and the local wind (Lass et al. 2001). The eastward barotropic main circulation in the north of the Odra estuary is very persistent dominating surface currents during spring and summer 2012 and summer 2013 (Fig. 5a, b, d) as well as respective bottom currents (Supplementary Figures S2a, b, d). Current velocities reduce drastically over the Odra bank initiating the transition to the wind-driven regime in the Pomeranian Bay (Figs. 1a and 5). The surface currents head mostly westward with recirculating flows at the bottom (Figs. 5e, f, h; S2a, b, d; Lass et al. 2001). The period of March–May 2013 differs from the general case with surface velocity vectors in the Pomeranian Bay heading to the North-West revealing dominance of easterly winds at the time (Fig. 5c, g). Due to the Ekman-type circulation within the stratified coastal boundary layer, bottom currents flow toward the shore in a southwestern direction during westerly winds (Fig. S2 e, f, h). These bottom currents play a role in transporting water from the Baltic Sea into the Greifswalder Bodden and towards the outlets of the lagoon (Fig. S2f, h) enhancing stratification even in relatively shallow areas with depth less than  $15 \text{ m}$  (Figs. 1a and 4f). The estuarine-type circulation occurs not only in the Pomeranian Bay but also in the mouth area of the Swina outlet as seen from arrows directed upstream into the Great Lagoon (Fig. S2h).

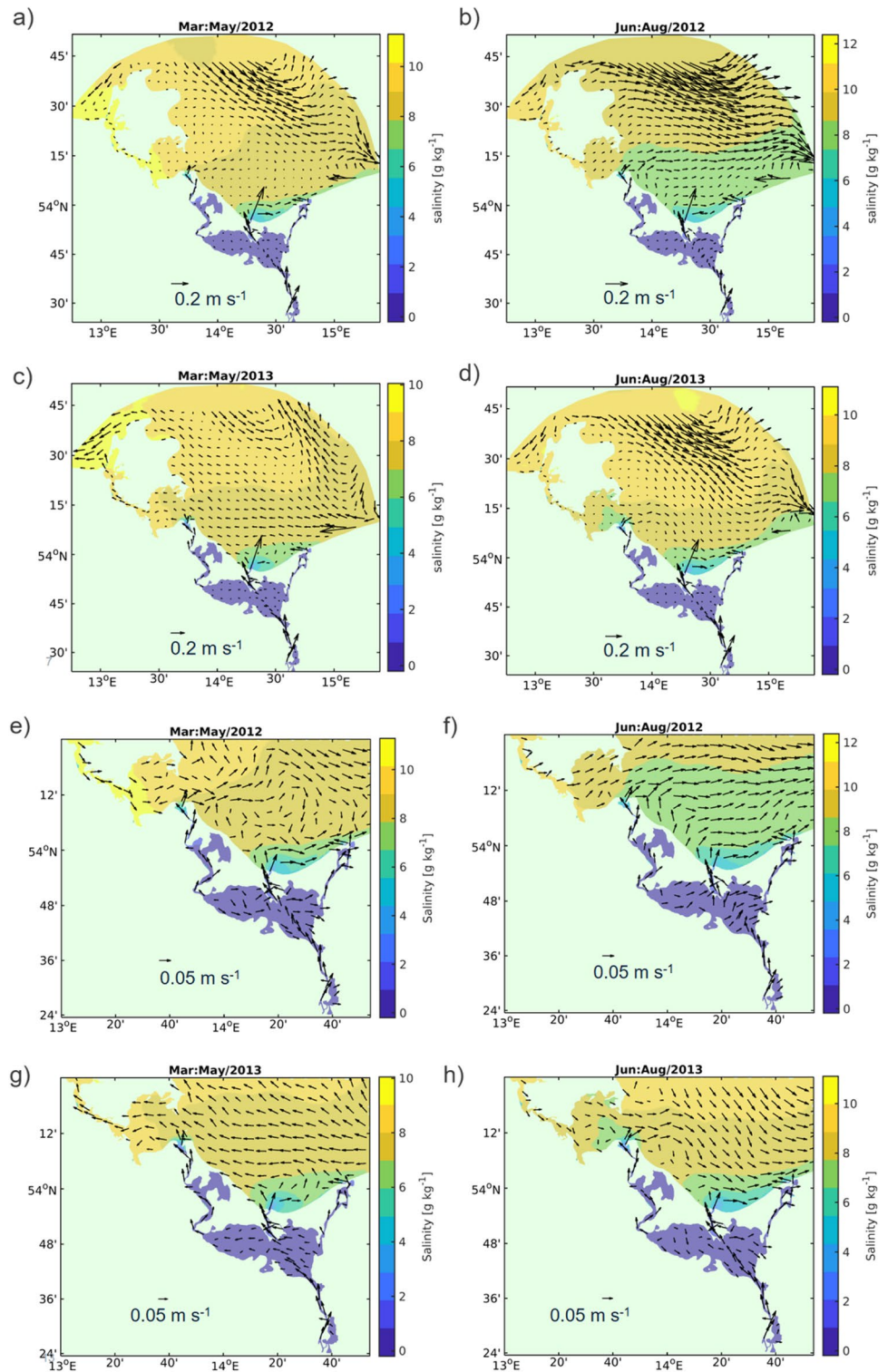
The results of the ocean model simulations evidence high realism when compared to observations. Additionally, they align with the principal circulation patterns documented in the existing literature while adding a couple of novel details to the overarching dynamic framework. In the following section, we elucidate the performance of the biogeochemical aspects of these simulations.

### 3.2 Connectivity and water age

The surface currents in the outlets reflect the average barotropic gradient between the Szczecin Lagoon and the Baltic proper. According to the model simulations, the average discharge of the Swina channel during 2012–2013 was  $489 \text{ m}^3 \text{ s}^{-1}$ . The Swina accounts for 73.5% of volume transport into the Baltic, followed by Peenestrom (15.7%) and Dziwna (10.8%). These numbers are similar but slightly different from Mohrholz and Lass (1998) who estimated the percentages of 69, 17 and 14 for Swina, Peenestrom and Dziwna, respectively. The volume transport through Swina and Peenestrom are closely correlated,



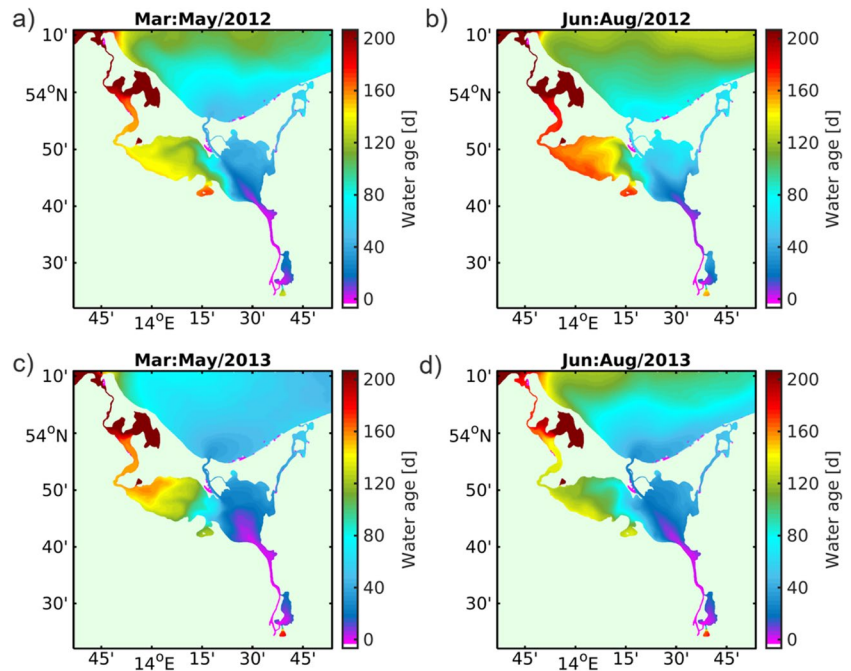
**Fig. 5** Average surface salinity and surface velocity vectors during **a** March-May and **b** June-August 2012, **c** March-May and **d** June-August 2013 where Supplementary figure S2a-d show respective bottom fields. **e-h** Zoomed-in view of Odra estuary average surface salinity and surface log velocity vectors during **e** March-May and **f** June-August 2012, **g** March-May and **h** June-August 2013, where Supplementary figure S2e-h show respective bottom fields



reflecting the similar and approximately zonal orientation of both outlets (Supplementary figure S3). The Dziwna outlets demonstrates a certain decoupling from Swina with both maximum positive (into the Baltic) and negative flows diverging from strictly linear relationship. One possible explanation to the special behavior of Dziwna is its

curvilinear geometry. For example, a westerly wind would drive the coastal current into the mouth of the channel, but also push water from the lagoon into the strait at its southern end, blocking water exchange. Straight northern or southern winds on the contrary would lead to efficient inflow or outflow, respectively.

**Fig. 6** Surface averages of water age from the model simulation are given for **a** March to May, 2012, **b** June to August, 2012, **c** March to May, 2013, **d** June to August, 2013



Related to the transports through the outlets and of utmost importance for the biogeochemical cycling is the residence time or water age. Friedland et al. (2019) found residence time in the Small Lagoon reaching 60 days whereas Schernewski et al., (2023) suggest Lagoon residence time could amount to three months. Using the water age tracer module available with the SCHISM (Shen and Haas 2004), we simulated the average water age assigning the freshwater entering the model area from Odra river age 0 days. Travelling with the flow, the water ages, mixing with neighboring water masses of distinct age. Figure 6 reveals average age tracer distributions during (a) spring 2012, (b) summer 2012, (c) spring 2013 and (d) summer 2013, whereas water entering at the southern most point at the model has age 0 days (Odra river, see Fig. 1b). The maps show that up to the lagoon proper at 53° 40' N, water age remains close to zero indicating short travelling time. In the lagoon, water age rises quickly with average age in the Great lagoon reaching 50 to 80 days in 2012 (Fig. 6a, b) compared to 20 to 40 days in 2013 Fig. 6c, d). The color scale in the Pomeranian Bay is almost identical with the one in the Great Lagoon demonstrating similar age of both water masses that apparently travel quickly from the Great Lagoon to the Pomeranian Bay. In the Small lagoon, water ages rise steeply in the central and western part reaching about 180 days in the summer of 2012 (Fig. 6b) contrasting with summer 2013 when age is about 120 days in the western part (Fig. 6d). The enhanced water age in the Small Lagoon is an indicator for long residence times and reveal a dynamical decoupling between the Small and the Great Lagoon.

### 3.3 Ecological dynamics

Time series of chlorophyll-a and nitrate illustrate the seasonal variability of the organic and inorganic loading of the Small Lagoon and Peenestrom (Fig. 7a–d). The observed chlorophyll concentrations reach up to 120 mg m<sup>-3</sup> and 80 mg m<sup>-3</sup> at the KHO station (Small Lagoon) and P20 station (Peenestrom), respectively (Figs. 7a, b; 1 b; Supplementary Table 1). The amplitude of simulated chlorophyll-a is similar, however the model results demonstrate phase differences and small-scale variability with prominent pulses beyond exceeding magnitude sparse observations. The observed nitrate concentrations collapse between end of April and beginning of July while the same happens between beginning of May and June the model simulations at the specific locations (Fig. 7c, d). The model thus captures the nitrate dynamics but slightly reduces the temporal range of the point of depletion.

The balance between autotrophic and heterotrophic processes and the transformation of organic matter to inorganic (mineralized) nutrients are reflected by the concentrations of dissolved oxygen and inorganic nitrogen. Taylor diagrams illustrate the model performance regarding these properties across in the area of the Small Lagoon, Peenestrom and Greifswalder Bodden (Fig. 8; for locations see Fig. 1a, b). They represent the same stations and are organized the same way as Fig. 3 above. The model demonstrates high realism simulating the oxygen variability in the Small Lagoon and the Greifswalder Bodden with correlation coefficients typically between  $R = 0.8$  and  $R = 0.9$  while normalized root-mean-square-errors do not exceed 0.6 mmol m<sup>-3</sup> (Fig. 8a).

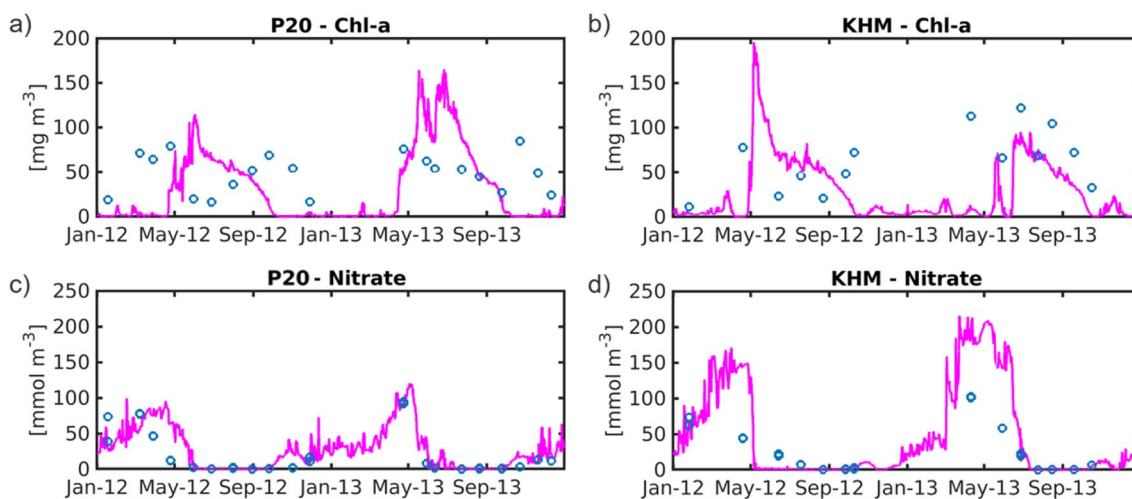
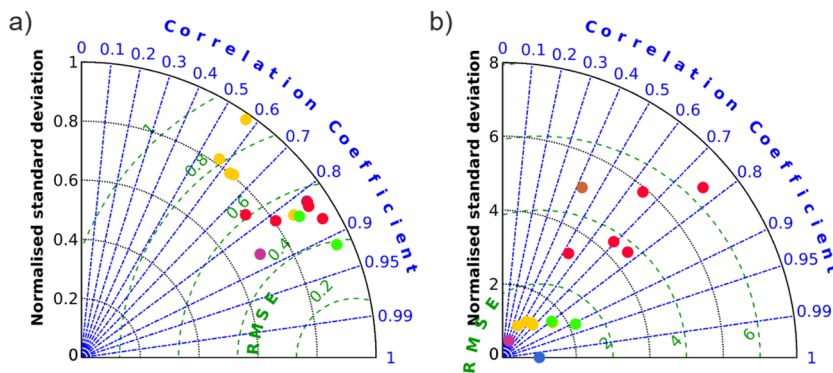


**Fig. 7** Comparison of simulated surface **a, b** chlorophyll-a and **c, d** nitrate concentrations against observations, where solid lines represent model results and blue circles represent measurements

**Fig. 8** Taylor diagrams of **a** surface oxygen and **b** surface dissolved inorganic nitrogen concentrations illustrate the agreement of model simulation with observation stations (see Fig. 1b) during 2012–2013

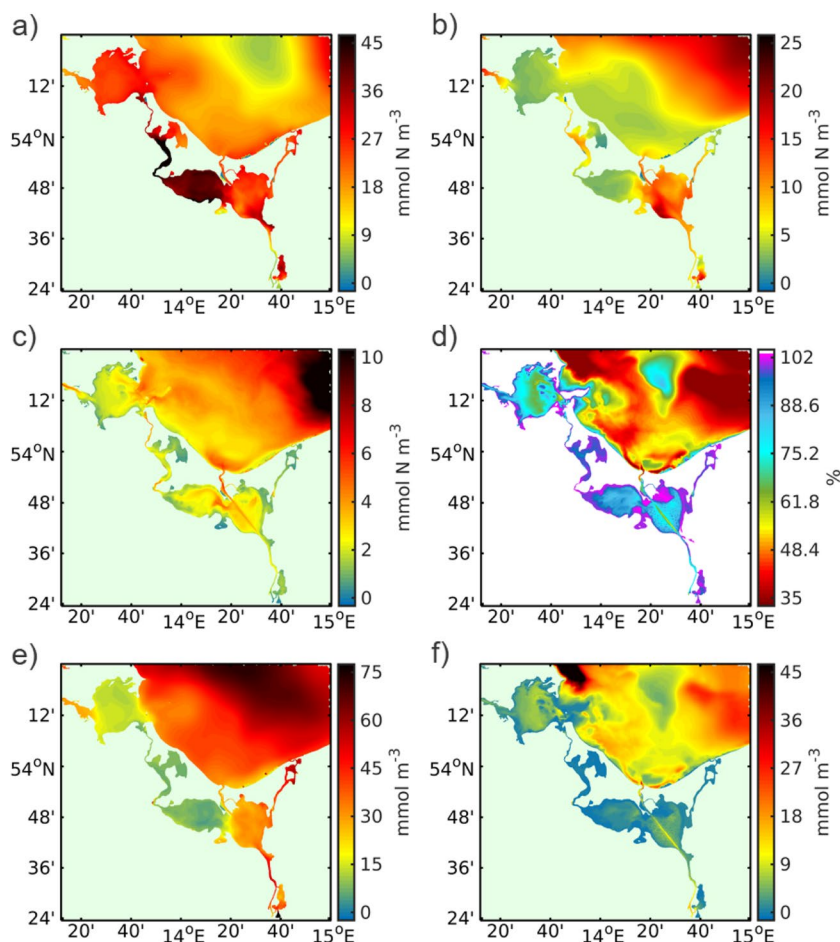


The ratio of simulated to observed oxygen variance is comparable everywhere including the Peenestrom. In this part of the system however correlation coefficients reach moderate  $R=0.6$  which might be due to phase differences between the simulated and observed signals. Dissolved inorganic nitrogen is tackled well in the inner parts of the Odra Lagoon with errors increasing in the Greifswalder Bodden (Fig. 8b). Still coefficients reveal at least moderate correlations between data and model at the majority of the stations. This comparison approves the overall realism of the biogeochemical simulation and the capability of the model to address the transformation of organic to inorganic nitrogen that is subsequently exported to the outer estuary and Baltic Sea.

Maps of phytoplankton nitrogen biomass, zooplankton nitrogen biomass, phyto-detritus nitrogen, bottom oxygen saturation, surface nitrate and bottom ammonium concentrations illustrate the spatio-temporal sequence of the biogeochemical cycling between the Odra river proper and the Baltic Sea (Fig. 9). Initial phyto biomass concentrations

at river boundary increase again upon reaching the Odra Lagoon (Figs. 9a, 1b). In the shallow waters of Odra estuary, average surface biomass nitrogen concentrations of primary producers during May to September 2012 are  $37.0 \text{ mmol N m}^{-3}$  in the Small Lagoon,  $25.8 \text{ mmol N m}^{-3}$  in the Great Lagoon,  $25.7 \text{ mmol N m}^{-3}$  in the Greifswalder Bodden and  $41.4 \text{ mmol N m}^{-3}$  in the Peenestrom, respectively (for geographical locations see Fig. 1). Respective portions of cyanobacteria biomass to total primary producers' biomass are 50%, 40%, 58% and 51%. Average zooplankton biomass concentrations are  $4.5 \text{ mmol N m}^{-3}$ ,  $11.5 \text{ mmol N m}^{-3}$ ,  $3.5 \text{ mmol N m}^{-3}$ ,  $6.3 \text{ mmol N m}^{-3}$  in the same basins, respectively. A tentative explanation for high phytoplankton biomass in the Small Lagoon and the Peenestrom is the high average water age in these regions in comparison with the Great Lagoon (Fig. 6). The latter in turn sees the highest biomass assemblages of large zooplankton that also tend to reduce phytoplankton biomass (Fig. 9b). According to the simulations the Peenestrom is the most productive and eutrophied part of the

**Fig. 9** Average pelagic concentrations of **a** phytoplankton nitrogen, **b** zooplankton nitrogen and **c** phyto-detritus nitrogen, **d** bottom oxygen saturation, **e** surface nitrate concentration, and **f** bottom ammonium concentration during May–September 2012. Supplementary figure S4 shows respective average fields during May–September 2013



Odra estuary system. The Greifswalder Bodden features almost the same average phytoplankton biomass as the Great Lagoon, which is an interesting result because this area does not receive any riverine nutrient forcing. In the Small Lagoon, the water age often exceeds that of its surroundings—the Peenestrom and Great Lagoon—by approximately thirty days (Fig. 6). Due to the shallower water depth, this does not significantly affect bottom oxygen saturation (Fig. 9d). In contrast, the coastal zone of the Pomeranian Bay displays widespread summer oxygen stress in the reference simulation of 2012 (Fig. 9d). Apart from the Odra bank, the outer estuary, and the adjacent Arkona basins, these regions exhibit hypoxic to anoxic bottom conditions, similar to those found in the deeper Baltic basins. The surface nitrate concentrations inversely reflect the pattern of phytoplankton biomass concentrations in the Odra estuary (Fig. 9a, e) with nitrate concentrations close to zero in the Small Lagoon and Peenestrom and elevated nitrate concentrations in Greifswalder Bodden and Great Lagoon. The bottom ammonium concentrations roughly follow the pattern of potential energy anomaly in the various sub-basins of the Odra estuary (Figs. 9f, 4 e, f) indicating additional fuelling of primary

production in the relatively deep or prone to stratification regions of the Greifswalder Bodden and Small Lagoon by remineralised ammonium.

A major stressor to many estuaries and lagoons connected to long eutrophied continental rivers are organic loads that break down upon reaching deeper coastal waters to be mineralized under the circumstances defined by the typical regional hydrodynamics. The Odra/Swina channel reveals a typical estuarine salinity and temperature gradient with average salinity increasing and average temperature decreasing from land to sea (Fig. 10a, b). A steep salinity front with a slope of  $\sim 0.6 \text{ g kg}^{-1} \text{ km}^{-1}$  marks the zone of the estuarine circulation and associated stratification (Fig. 10a, Supplementary figure S5). A plume of relatively warm river-borne water covers the salty and cooler bottom waters indicating control of stratification by differential advection of both salinity and temperature gradients. From transect km 40 (Fig. 1a) upstream the Lagoon is freshwater-dominated. Vertical temperature gradients explain the stratification detected in the same area (Figs. 10b, 4 f). In effect, the navigational channel connecting Odra river and Pomeranian Bay via the Swina outlet comprises three distinct physical zones, as reflected by the along-channel transect of  $\phi$  (Eq. 2;

**Fig. 10** Along-channel profiles of average **a** salinity, **b** temperature, **c** diatom nitrogen, **d** flagellate nitrogen, **e** nitrogen ammonium, **f** particulate organic nitrogen (phyto-detritus), **g** nitrogen nitrate, **h** dissolved oxygen concentration in the Svina channel during May to September 2012. Supplementary figure S6 shows respective profiles during May–September 2013

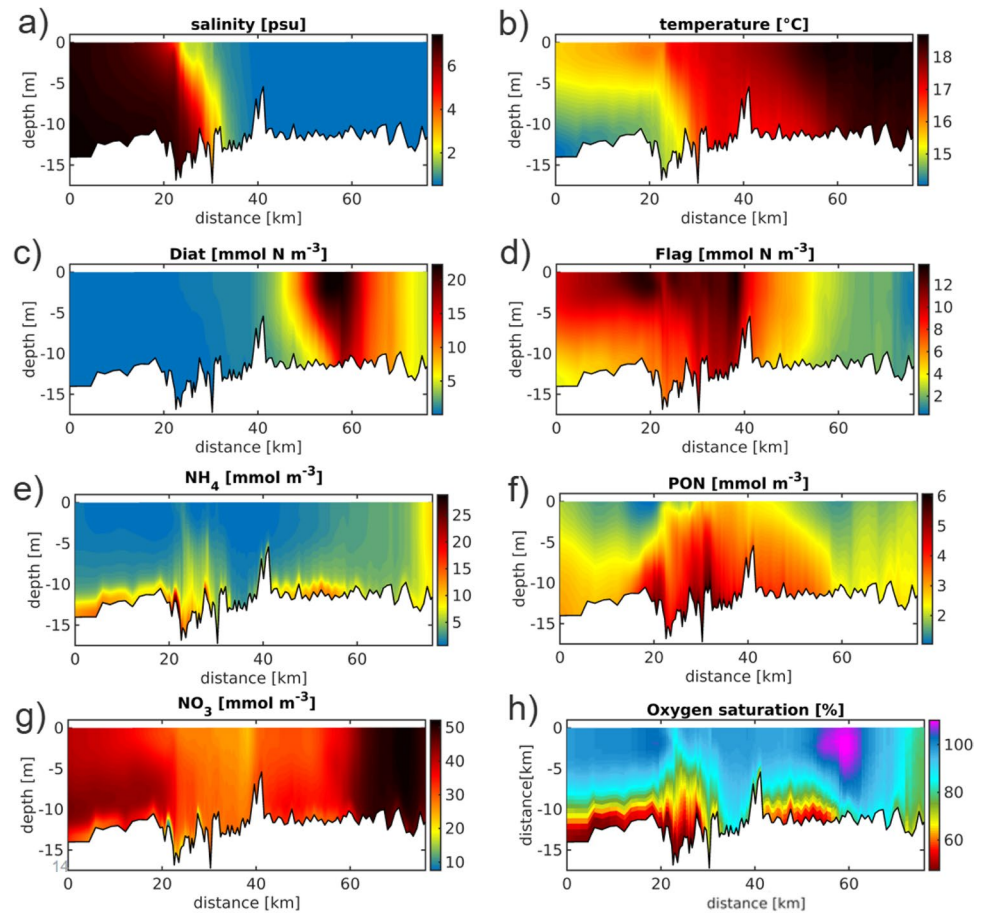


Fig. S5): Mildly stratified brackish coastal zone, stratified estuarine density front, and the freshwater zone with average  $\phi$  close to zero.

The thermally stratified central lagoon waters provide the best conditions for primary producers (Fig. 10c, d). The primary producer concentrations sharply decrease towards the salinity front which is thus also a biological front. The dead planktonic material distributes along the transect near the bottom (Fig. 10e). Ammonium from the mineralization of the particulate organic material is taken up in the area of high primary producer concentrations and accumulates in the area of the brackish inflow (Fig. 10f). Near the sea bed, nitrate and oxygen concentrations reduce indicating denitrification outside the lagoon (Fig. 10g, h).

In order to quantify the relationships between water age, stratification and nitrogen dynamics described above, Supplementary figure S7 shows the linear correlation coefficients between water temperature, water age and potential energy anomaly on the one hand and near-bottom oxygen concentration, near-bottom ammonium concentration, near-bottom ammonium concentration and nitrogen dynamics on the other. Unsurprisingly, the near-bottom oxygen concentration decreases with increasing temperature. In contrast, the oxygen values are proportional to the water age in the area

of the Small Lagoon and partly in the Greifswalder Bodden and anti-proportional in the narrow Peenestrom, which hampers a clear interpretation. In contrast, increasing stratification clearly leads to decreasing near-bottom oxygen levels at stations nr. 1, 2, 3, 4, 6, 12 and 13 (see map in Fig. 1b). At the same locations, there is a positive correlation between stratification and near-bottom ammonium concentration, which indicates a dynamic inhibition of nitrification due to oxygen deficiency under the stratified water column. At stations nr. 4, 5 and 6, there is a mild positive correlation between stratification and denitrification rates. Stations nr. 2, 4 and in particular station 5 show negative correlation coefficients between water age and denitrification rates indicating increasing unavailability of nitrate nitrogen. However, it should not be overlooked that in shallow waters, even under summer conditions, the oxygen content is often too high to allow for denitrification.

### 3.4 Climate change sensitivity experiment

To quantify the reponse of the Odra lagoon system to aspects of projected climatic change, the model run has been repeated as simplified climate change experiment (see Sect. 2.4). As a result, the surface temperature in the model

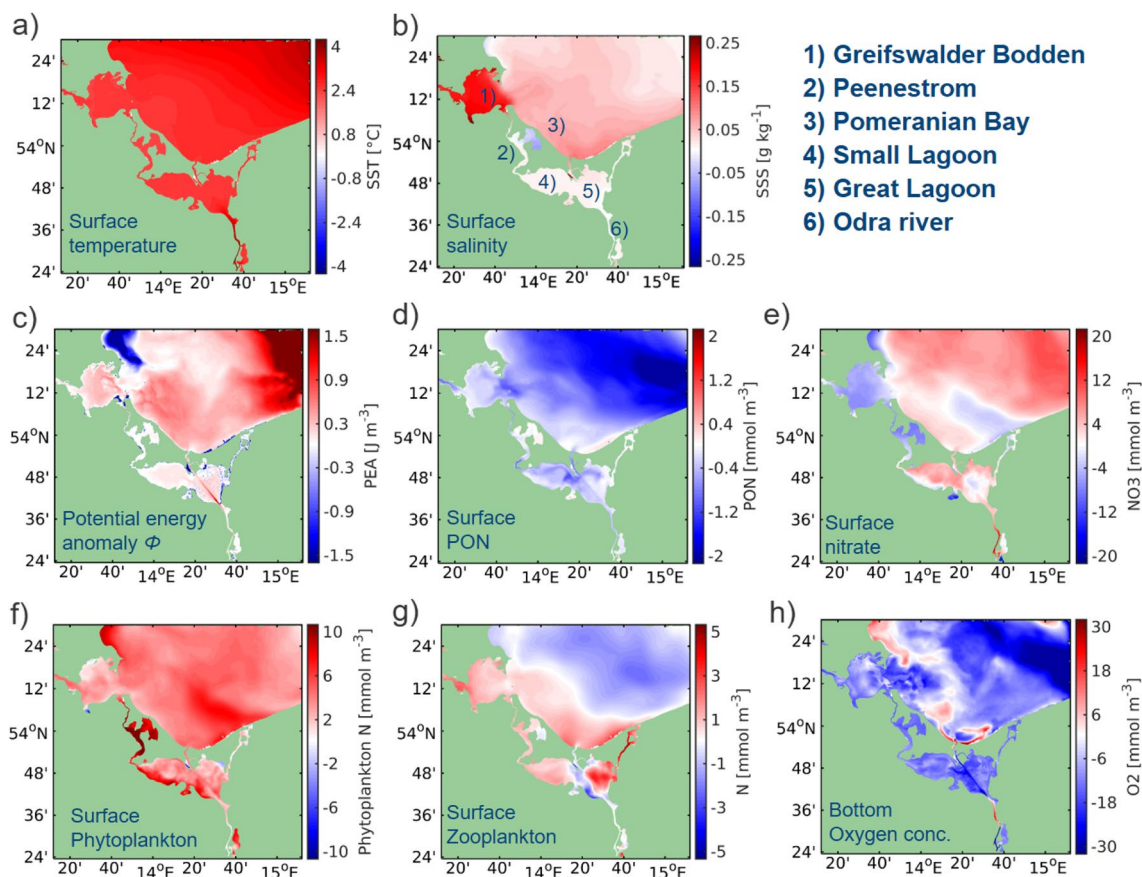


**Fig. 11** Spatial changes of physical and biogeochemical properties in the focal region under a climate change sensitivity experiment showing differences of **a** sea surface temperature [ $^{\circ}\text{C}$ ], **b** sea surface salinity [ $\text{g kg}^{-1}$ ], **c** potential energy anomaly [ $\text{J m}^{-3}$ ], **d** surface particulate organic nitrogen (PON) [ $\text{mmol m}^{-3}$ ], **e** surface nitrate [ $\text{mmol m}^{-3}$ ], **f**

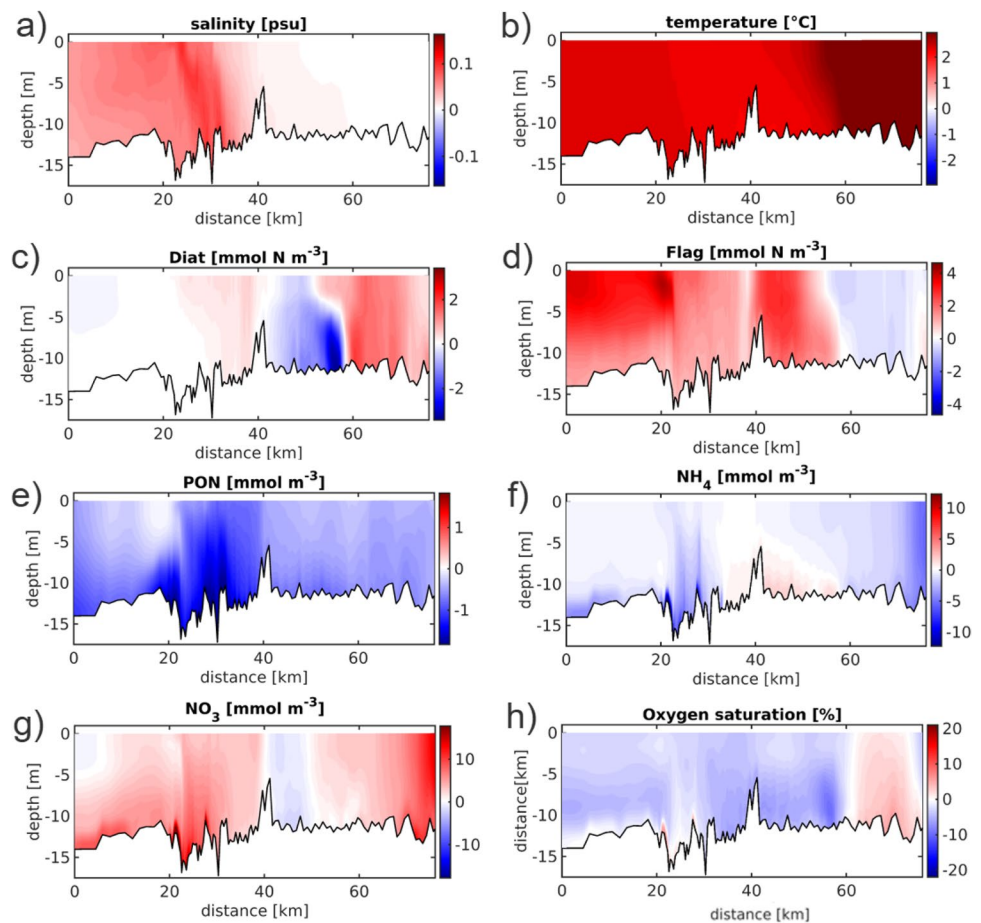
surface phytoplankton biomass nitrogen [ $\text{mmol m}^{-3}$ ], **g** surface zooplankton biomass nitrogen [ $\text{mmol m}^{-3}$ ], **h** bottom oxygen concentration [ $\text{mmol m}^{-3}$ ]. **b** indicates locations of geographical names used in the figure discussion. Supplementary figure S8 shows respective differences during May–September 2013

area has increased by at least  $2^{\circ}\text{C}$  (Fig. 11a). By force of the higher water temperature, reduced density and enhanced evaporation fluxes led to an increase in salinity in the Pomeranian Bay and the Greifswald Bodden, where the maximum change reached  $0.25\text{ g kg}^{-1}$  (Fig. 11b). Sea level rise, changes to the thermohaline field impact on density stratification that increases throughout the Odra estuary system, particularly in the deeper regions such as the shipping channel in the Great lagoon and the Pomeranian Bay (Fig. 11c, see Fig. 11b for geographical information). Since the process rates of remineralisation, nitrification and denitrification are directly temperature-dependent the whole lower-trophic level ecosystem dynamics are very likely affected.

Indeed the model experiment showed a global reduction of phytodetritus concentration (Fig. 11d), which was more than  $2\text{ mmol m}^{-3}$  in the deeper Baltic Sea, but barely reached  $0.5\text{ mmol m}^{-3}$  in the shallow lagoon and the Bodden. The reduction in particulate organic matter was mirrored by an increase in nitrate concentration in most of the model area (Fig. 11e). Only the northern part of the Peenestrom and the

Greifswalder Bodden showed a reduction in nitrate concentration in the climatic model experiment. The most striking response of the experiment, however is the clear increase in the density of primary producers, which amounts to up to  $10\text{ mmol N m}^{-3}$  in the Peenestrom (Fig. 11f). With a maximum of  $40\text{ mmol N m}^{-3}$  in the reference case, this means an increase of up to 25% locally. The increase in primary producers automatically means better conditions for the zooplankton, which consequently also increase (Fig. 11g). Due to the higher process rates in the respiration of detritus, the bottom oxygen content in the experiment decreases globally compared to the reference case revealing small scale structures along the coastline (Fig. 11h). Obviously higher concentration of primary producers compensate for this locally. A narrow coastal strip at the outflow of the Swina, the east coast of Rügen Island and the Odra in the southern part of the lagoon show higher oxygen concentrations down to the bottom layer. Both the—much more widespread—decrease and the local increase in oxygen content are in the order of up to  $30\text{ mmol m}^{-3}$ .

**Fig. 12** Along-channel profiles of differences between the climate experiment and reference run of (a) salinity, (b) temperature, (c) diatom nitrogen, (d) flagellate nitrogen, (e) particulate organic nitrogen (PON), (f) ammonium, (g) nitrate and (h) oxygen saturation along the transect depicted in Fig. 1b. All profiles represent averages of May to September 2012 in reference run and climate sensitivity experiment, respectively. Supplementary figure S9 shows respective differences during May–September 2013



These changes are also evident along the canal through the Great Lagoon and the Swina. The warming of the lagoon water in the experiment is between 2 °C in the lower and middle part of the transect and increases to almost 3 °C towards the Odra river (Fig. 12b). In the area of the brackish water front, salinity increases by up to 0.1 g kg<sup>-1</sup>, with the pattern of change reflecting typical gravity circulation, with an advance of the saltier, heavier water at the bottom (Fig. 12a). The concentration of the two phytoplankton groups also largely increases, especially flagellates (Fig. 12c, d). Diatoms increase especially in the upper part of the transect in the southern Great Lagoon, while there is a decrease in the northern part of the Great Lagoon. This is due to an increase in zooplankton in this area (not shown), which increases the grazing pressure.

Despite the increase in plankton in the lagoon and along the Swina, the concentrations of organic particulate matter are declining (Fig. 12e), with the decline being particularly pronounced around the salinity front. It is easy to see how the strengthening of the gravitational circulation both increases the salinity locally and amplifies global biological trends—here the decrease in particulate organic material under enhanced by global warming remineralization rates.

Ammonium concentrations decrease in the same area and at the bottom of the Pomeranian Bay (km 0 to km 30, Fig. 12f). One might expect an increase in ammonium concentrations due to the enhanced remineralization rates, however nitrification gets enhanced as well increasing nitrate concentrations almost globally along the transect (Fig. 12g). Locally, in the area of strong phytoplankton blooms in the central part of the Great Lagoon, change in nitrate is negative indicating depletion of the nutrient. Enhanced remineralisation and nitrification increase oxygen depletion along most of the transect between km 0 and km 60. Upstream increase of primary producers compensates the global trends inducing positive change of oxygen saturation in the climatic experiment of approximately 5% (Fig. 12h).

Hypoxic area of the total model domain reaches up to 4.476e9 m<sup>2</sup> in 2012 and up to 4.339e9 m<sup>2</sup> in 2013 of the reference simulation. In the climatic change experiment, these numbers change to 4.451e9 m<sup>2</sup> and 4.383e9 m<sup>2</sup>, respectively. The number of days with an area greater than 1e9 m<sup>2</sup> affected by hypoxia equals 105 days for both the hind-cast run of 2012 and the climatic change experiment. In contrast, this period increases from 145 to 160 days for 2013. In Odra Lagoon, no hypoxia occurs in both

**Fig. 13** Monthly sum of fluxes of **a** inorganic nitrogen (DIN) and **c** organic nitrogen (ON) from the three lagoon outlets to the Baltic proper, **b, d** differences between lagoon inflow from Odra river outflow to the Baltic Sea of DIN and ON, respectively. Hovmoeller diagrams of **e** nitrate and **f** along the Great Lagoon (see transect in Fig. 1b) illustrate the dynamical background of the nutrient exports

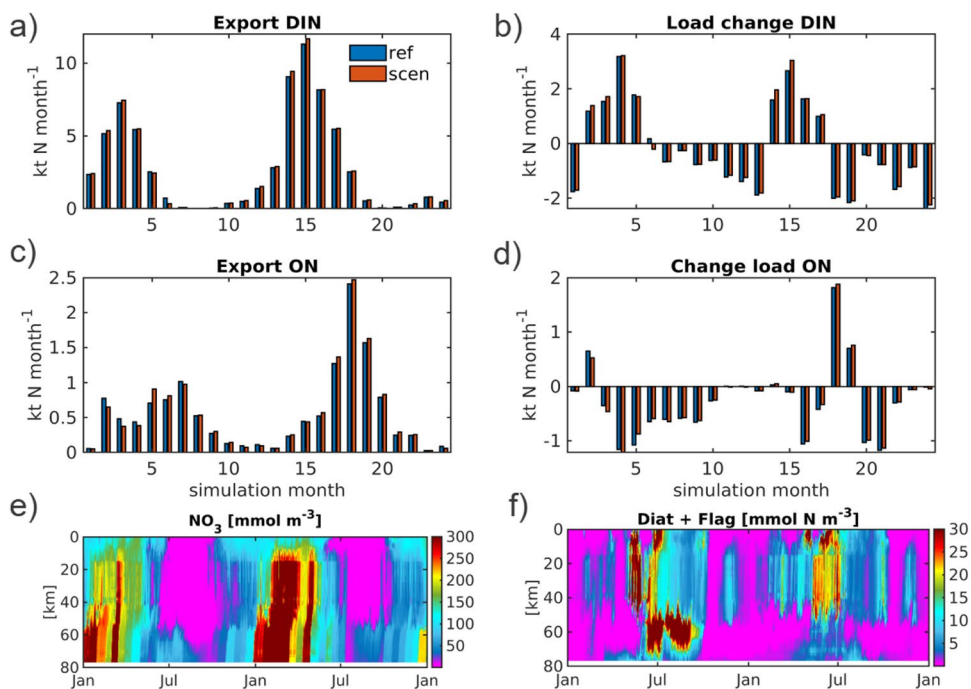


**Table 1** Riverine total nitrogen fluxes into Odra Lagoon (1st column,  $N_{tot\_in}$ ), total nitrogen fluxes from the Odra Lagoon outlets to the Baltic (2nd column,  $N_{tot\_out}$ ), percent change between total nitrogen inflow and outflow (3rd column, Change), nitrogen denitrification in Odra Lagoon (4th column, Denitrif.), total nitrogen residual between inflow, outflow and denitrification (5th column, Residual),

annual nitrogen uptake by primary production including nitrogen fixation by cyanobacteria (6th column, Prim. prod.) and annual ammonium release from sedimentary layer (7th column,  $NH_4$  release) are given for 2012 and 2013 of the reference run (1st and 2nd row) and of the climate scenario run (3th and 4th row), respectively

	$N_{tot\_in}$ [ktN/a]	$N_{tot\_out}$ [ktN/a]	Change [%]	Denitrif. [ktN/a]	Residual [ktN/a]	Prim. prod. [ktN/a]	$NH_4$ release [ktN/a]
2012_ref	34.82	31.16	-10.49	4.32	-0.67	47.12	2.43
2013_ref	56.38	49.36	-12.46	1.68	5.34	45.02	0.88
2012_scen	34.82	31.37	-9.9	4.7	-1.25	67.96	2.48
2013_scen	56.38	50.92	-9.68	2.07	3.39	67.18	1.02

reference simulation and climatic experiment in 2013. In 2012, maximum hypoxic area reached  $9.558e4 \text{ m}^2$  in the reference simulation and even  $4.414e6 \text{ m}^2$  in the climatic change experiment. These results demonstrate that in the Odra Lagoon conditions of climatic change may drastically increase the area affected by hypoxia. In contrast, the effect of climatic change in the total model domain on area affected by hypoxia is about 1% only. This means that under the forcing conditions of 2012, the climatic change experiments leads to spatial spreading of hypoxia in the shallow Odra Lagoon whereas spatial response in the Baltic proper is relatively mild. Under the forcing conditions of 2013 that includes a summer river flood, the Odra Lagoon remains unaffected by hypoxia while hypoxic area and hypoxic period increase in the outer waters of the Odra estuary and Baltic proper.

### 3.5 Nitrogen export to the Baltic

Finally, we discuss the simulated seasonal and annual fluxes from the shallow coastal lagoon to the Baltic basin in hind-cast and climate change experiment. The nitrogen fluxes from the Odra Lagoon into the Baltic proper via the three outlets reveal a strong seasonality with a typical phase difference between inorganic and organic nitrogen fluxes (Fig. 13a, c). According to the model simulations, the exports of inorganic nitrogen and organic nitrogen in 2012 amount to 26.1 kt and 5.4 kt, respectively. In 2013 the exports are 42.6 kt and 8.2 kt of inorganic and organic nitrogen. The annual total nitrogen imports into and exports from the Odra Lagoon are given in Table 1. The interannual variation of total nitrogen fluxes is roughly proportional to the one of Odra river discharge, which was  $465.7 \text{ m}^3 \text{ s}^{-1}$  in 2012



and  $659.4 \text{ m}^3 \text{ s}^{-1}$  in 2013 suggesting that river discharge is a dominant driver of nitrogen exports. An earlier study estimated annual total nitrogen exports from Odra estuary the Baltic Sea to amount to approximately 44 kt N in the period of 1993–1998 (Pastuszak et al. 2005). This number is close to our calculation of total nitrogen exports for 2013 while clearly exceeding the one for 2012. Apart from inter-annual variability, this discrepancy is likely explained by higher riverine nitrogen loads of more than  $70 \text{ kt N yr}^{-1}$  at the time. Furthermore, these authors found a nitrogen retention of 45% in the Odra Lagoon estuary system while – different from this study – including the southern part of the Pomeranian Bay into their calculations. Here we find that the amount of nitrogen retention in the Odra Lagoon including its outlets equals roughly 10% per annum (Table 1). Model results imply that nitrogen retention decreases slightly between 1.5 and 2.4% under conditions of climatic change experiment. This is despite an increase of denitrification in both 2012 and 2013 under the climatic change experiment. The “dry” year 2012 reveals ~2.5 times of denitrified nitrogen in comparison to the “wet” year 2013. The latter ends with a higher total nitrogen residual, i.e. the amount of nitrogen remaining in the lagoon at the end of the year mostly in the sedimentary layer, reflecting small amount of denitrified nitrogen in relation to the nitrogen inflow. Figure 13b shows the nitrogen sink to be particularly active during the winter months when activity of primary producers is low.

Low primary production in early spring would also explain the seasonal high of increase of inorganic nitrogen fluxes upon passing the Odra Lagoon (Fig. 13c). These modifications of inorganic nitrogen fluxes inside the lagoon appear to be similar in timing and magnitude during 2012 and 2013, respectively. Furthermore, the amount of nitrogen assimilated during primary production is very similar for both run years (Table 1). Primary production however intensifies under conditions of climate change which can be explained by enhanced nutrient recycling rates and increased by ~25% water depth and volume. We remind here that Odra Lagoon is known for its high primary production that according to Stokowski et al. (2020) and cited therein studies may assimilate 90–100% of the nitrogen inputs while carbon fixation may locally exceed  $600 \text{ mg C m}^{-2}$ . Here we find an average of  $382 \text{ mg C m}^{-2}$  carbon fixated in the inland waters of the Odra estuary in the reference simulation whereas in the climatic change experiment this value increases to  $559 \text{ mg C m}^{-2}$ . The increase of organic uptake could be a major reason for the decrease of relative nitrogen retention capacity in the climatic change experiment because of enhanced nitrogen fixation by cyanobacteria plus accelerated uptake of inorganic nitrogen by oxygen-emitting phytoplankton. The latter process hampers efficient upscaling of denitrification with rising temperatures that negatively impacts the nitrogen retention capacity of the lagoon.

The timing of change of organic nitrogen fluxes is very different in 2012 compared to 2013 (Fig. 13d). This is mainly due to increased river discharge between May and July 2013 reaching more than  $1300 \text{ m}^3 \text{ s}^{-1}$  end of June and beginning of July. The flood peaks coincide with release of organic nitrogen including plankton and phyto-detritus to the Baltic. Clearly the flushing of the Odra Lagoon hampered internal cycling of nitrogen decreasing chances for denitrification. Table 1 confirms relatively low recycling of ammonium from the Lagoon sedimentary layer in 2013 compared to 2012 under conditions of both reference simulation and climatic change experiment. Accordingly, Fig. S4f reveals clearly lower bottom ammonium concentrations in Odra Lagoon than corresponding Fig. 9f, whereas Fig. S4e reveals elevated nitrate concentration in the lagoon counter-indicating nitrate depletion in summer 2013. Meanwhile, bottom oxygen levels have decreased widely in the Pomeranian Bay and Baltic proper in Fig. S4d compared to Fig. 9d supporting the hypothesis of organic material being flushed into the regional ocean during the high-runoff events.

Finally, Hovmoeller diagrams of surface nitrate, the main dissolved inorganic nitrogen species, and phytoplankton nitrogen illustrate the dynamical background of the nitrogen fluxes (Fig. 13e, f). At times of almost zero exports of inorganic nitrogen, the nitrate inputs to the lagoon get depleted already around km 60 of the transect (Figs. 13a, e, 1 b). During these period in June to August 2012 and from June on in 2013, inorganic nitrogen balance in the lagoon is negative (Fig. 13b). Whereas in 2013 the nitrogen is taken up by primary producers leaving the lagoon in the form of organic nitrogen, it seems that in 2012 the nutrient fizzles out. We remind here that in 2012 not only river discharge was smaller but also water age was higher than in the second year of the simulations (see Fig. 6), posing favorable conditions for nitrogen to end up in the denitrification pathway. The June 2013 river flood with peak discharge of  $\sim 1370 \text{ m}^3 \text{ s}^{-1}$  is associated with enhanced phytoplankton biomass along the transect in the area of the Great Lagoon and the Pomeranian Bay as well as a surge in organic matter exports to the Baltic (Fig. 13b, f). A preliminary deduction can be drawn that the lagoon's flushing resulting from a river flood fosters favorable conditions for plankton blooms, which are then exported to the Baltic proper. This dual effect reduces the lagoon's buffering capacity and diminishes the potential for denitrification within its confines.

## 4 Conclusion and outlook

For a deeper understanding of the importance of eutrophication and internal nitrogen cycling in estuarine shallow water areas for nutrient export and thus eutrophication impacts in the adjacent regional ocean, this study used a high-resolution

coupled physical-biogeochemical model of the Odra Lagoon estuarine system and adjacent Baltic Sea. The simulations included both a two-year hindcast and a climate experiment with altered water level and temperature influences. The hind-cast reliably reproduced stationary measurements of salinity and water temperature in shallow water. The biogeochemical simulation was convincing with accurate magnitudes of chlorophyll-*a* and inorganic dissolved nitrogen. The seasonal phase of biogeochemical variability was more difficult to model, but showed convincing results—especially with respect to dissolved inorganic nitrogen. Thus, the model proved a suitable tool for estimating nitrogen exports from shallow water areas to the Baltic Sea. It was shown that these mainly occur in the cold season, while even during winter time nitrogen sinks appeared to be active in the shallow waters of the Odra Lagoon. In the productive season, primary producers completely depleted inorganic nitrogen, such that inorganic nitrogen exports to the regional Baltic Sea faded out. In 2012 the amount of nitrogen fixed by primary production even exceeded riverine nitrogen inputs evidencing internal cycling of nitrogen. This means that potentially Odra Lagoon is an important source for organic nitrogen for the Baltic proper. In the dry year 2012 however, this was hardly the case due to stagnating discharges and high water age, especially in the Small Lagoon. In the wet year 2013, which was also characterised by an extreme river flood in summer, relatively large amounts of organic material were flushed into the Baltic Sea, which is in good agreement with reports from the literature. For future work, it will be of interest to understand at which threshold values of discharge and water age or residence time the internal storage and rearrangement is interrupted, so that a strong export of organic nutrients is initiated.

This study revealed the typical seasonal cycles of organic and inorganic nitrogen variability and the associated exports to the Baltic through the Odra Lagoon outlets. The annual nitrogen exports to the Baltic principally agreed with the reported literature values taking into account that the years 2012 and 2013 fall in the period of decreasing nitrogen inputs. Nitrogen retention was lower than reported previously (Pastuszak et al. 2005) which may be due to underrepresentation of denitrification in deeper, hypoxic sediment layers not represented by the model used herein. On the other hand it is also plausible that nitrogen has become increasingly limiting – as recently suggested (Schernewski et al. 2023) – instigating competition between primary producers and denitrifiers (for nitrate) hampering the denitrification and retention capacity of the lagoon. A climate change experiment showed a strong increase in primary producers, serving as a clear indicator of increasing eutrophication. At the same time, the hypoxic area multiplied in Odra Lagoon relative to the reference simulation of 2012. The enhanced primary production under conditions of climatic change may further threaten the

ecological status of deeper areas receiving their outflow in the future. This was evident from the model simulations showing oxygen levels decreased significantly already by reaching the Pomeranian Bay of the Baltic Sea. In consequence, the nitrate near the ground was depleted in the area of the stratified Odra plume indicating enhanced denitrification. Apart from the very shallow areas of 2–5 m depth, the deeper but meandering channels like the Swina exhibited remarkable resilience against decrease in oxygen. This resilience can be attributed to the sea level rise in the climate experiment, which enhanced currents and instigated a more vigorous overturning circulation through the curvature of the channel. Overall, the climate experiment's effects were consistent with anticipated impacts on shallow and deep regions, yielding recognizable patterns. Nutrient exports did not shift dramatically, however the annual nitrogen retention in the Odra Lagoon decreased slightly in climatic change experiment relative to reference run. A tentative explanation is that climate-enhanced primary production hinders nitrogen retention through denitrification via competition for available nitrogen nitrate and oxygen production. This means that shallow water environment like the Odra Lagoon is able to pass the burden of climatic change to the regional ocean. It is crucial to acknowledge that the assessment of land-side climate impacts was omitted in this study. Future analyses would necessitate the inclusion of these factors for a more comprehensive understanding of the intricate interplay between physical and biogeochemical dynamics in response to evolving climate conditions.

**Supplementary Information** The online version contains supplementary material available at <https://doi.org/10.1007/s10236-024-01607-w>.

**Acknowledgements** The authors are grateful to Dr. Ute Daewel (Hereon) for providing the ecological boundary forcing in the Baltic Sea, to Dr. Clemens Engelke and Mario von Weber (LUNG Mecklenburg-Vorpommern) for providing observational data in the area of Odra estuary and to the Waterway administration of Szczecin for providing bathymetric data of Odra, Swina and Dzwina channels. JP thanks BluEs consortium for fruitful discussions and acknowledges funding by the BMBF project BluEstuaries (BluEs) of the KüNo program, grant number 03F0864C. The authors acknowledge Horizon Europe Project Edito Model lab (Grant Agreement 101093293). JS acknowledges DOORS project (Grant Agreement 101000518) and HGF project SeaReCap. JP acknowledges NAPSEA project (Grant Agreement 101060418). This work profited from and contributed to the methodical development and aims of the CLICCS excellence cluster funded by German Research Association (DFG).

**Funding** Open Access funding enabled and organized by Projekt DEAL. Bundesministerium für Bildung, Wissenschaft, Forschung und Technologie, 03F0864C, Johannes Pein

**Data availability** The raw data supporting the conclusions of this article will be made available by the authors without undue reservation.

## Declarations

**Conflict of interest** The authors declared that they have no conflict of interest.

**Open Access** This article is licensed under a Creative Commons Attribution 4.0 International License, which permits use, sharing, adaptation, distribution and reproduction in any medium or format, as long as you give appropriate credit to the original author(s) and the source, provide a link to the Creative Commons licence, and indicate if changes were made. The images or other third party material in this article are included in the article's Creative Commons licence, unless indicated otherwise in a credit line to the material. If material is not included in the article's Creative Commons licence and your intended use is not permitted by statutory regulation or exceeds the permitted use, you will need to obtain permission directly from the copyright holder. To view a copy of this licence, visit <http://creativecommons.org/licenses/by/4.0/>.

## References

- Benkort D, Daewel U, Heath M, Schrum C (2020) On the role of biogeochemical coupling between sympagic and pelagic ecosystem compartments for primary and secondary production in the Barents Sea. *Front Environ Sci* 8:217. <https://doi.org/10.3389/fenvs.2020.548013>
- Bruggeman J, Bolding K (2014) A general framework for aquatic biogeochemical models. *Environ Model Softw* 61:249–265. <https://doi.org/10.1016/j.envsoft.2014.04.002>
- Chojnacki JC (1999) Description of Ecosystem of the Lower Odra and the Odra estuary. *Acta Hydrochim Hydrobiol* 27(5):257–267. [https://doi.org/10.1002/\(SICI\)1521-401X\(199911\)27:5%3c257::AID-AHEH257%3e3.0.CO;2-V](https://doi.org/10.1002/(SICI)1521-401X(199911)27:5%3c257::AID-AHEH257%3e3.0.CO;2-V)
- Daewel U, Schrum C (2013) Simulating long-term dynamics of the coupled North Sea and Baltic Sea ecosystem with ECOSMO II: model description and validation. *J Mar Syst* 119:30–49. <https://doi.org/10.1016/j.jmarsys.2013.03.008>
- Daewel U, Schrum C (2017a) Low-frequency variability in North Sea and Baltic Sea identified through simulations with the 3-D coupled physical–biogeochemical model ECOSMO. *Earth Syst Dynam* 8:801–815. <https://doi.org/10.5194/esd-8-801-2017>
- Daewel U, Schrum C (2017b) ECOSMO II hindcast simulations for the North Sea and Baltic Sea (1948–2008). World Data Center for Climate (WDCC) at DKRZ. 10.1594/WDCC/ECOSMOII\_NCEP.1948-2008
- Deborde J, Anschutz P, Aubry I, Glé C, Commarieu MV, Maurer D, ... Abril G (2008) Role of tidal pumping on nutrient cycling in a temperate lagoon (Arcachon Bay, France). *Mar Chem* 109(1–2):98–114. <https://doi.org/10.1016/j.marchem.2007.12.007>
- Friedland R, Schernewski G, Gräwe U, Greipsland I, Palazzo D, Pastuszak M (2019) Managing eutrophication in the Szczecin (Odra) lagoon-development, present state and future perspectives. *Front Mar Sci* 5:521. <https://doi.org/10.3389/fmars.2018.00521>
- Grinsted A, Jevrejeva S, Riva RE, Dahl-Jensen D (2015) Sea level rise projections for northern Europe under RCP8.5. *Clim Res* 64(1):15–23. <https://doi.org/10.3354/cr01309>
- Hosseini ST, Stanev E, Pein J, Valle-Levinson A, Schrum C (2023) Longitudinal and lateral circulation and tidal impacts in salt-plug estuaries. *Front Mar Sci* 10:1152625. <https://doi.org/10.3389/fmars.2023.1152625>
- Kaspar F, Niermann D, Borsche M, Fiedler S, Keller J, Potthast R, Rösch T, Spangehl T, Tinz B (2020) Regional atmospheric reanalysis activities at Deutscher Wetterdienst: review of evaluation results and application examples with a focus on renewable energy. *Adv Sci Res* 17:115–128. <https://doi.org/10.5194/asr-17-115-2020>
- Kjerfve B (1986) Comparative oceanography of coastal lagoons. In: *Estuarine variability*, pp 63–81. Academic Press. <https://doi.org/10.1016/B978-0-12-761890-6.50009-5>
- Kowalewska-Kalkowska H (2021) Storm-surge induced water level changes in the Odra river mouth area (southern baltic coast). *Atmosphere* 12(12):1559. <https://doi.org/10.3390/atmos12121559>
- Kowalewska G, Konat-Stepowicz J, Wawrzyniak-Wydrowska B, Szymczak-Żyła M (2003) Transfer of organic contaminants to the Baltic in the Odra Estuary. *Mar Pollut Bull* 46(6):703–718. [https://doi.org/10.1016/S0025-326X\(03\)00062-6](https://doi.org/10.1016/S0025-326X(03)00062-6)
- Lass HU, Mohrholz V, Seifert T (2001) On the dynamics of the Pomeranian Bight. *Cont Shelf Res* 21(11–12):1237–1261. [https://doi.org/10.1016/S0278-4343\(01\)00003-6](https://doi.org/10.1016/S0278-4343(01)00003-6)
- LUNG (2016) Monitoringprogramm zur Überwachung der Oberflächengewässer und des Grundwassers in Mecklenburg-Vorpommern im Zeitraum 2016–2021
- Meier HEM, Dieterich C, Eilola K et al (2019) Future projections of record-breaking sea surface temperature and cyanobacteria bloom events in the Baltic Sea. *Ambio* 48:1362–1376. <https://doi.org/10.1007/s13280-019-01235-5>
- Mohrholz V, Lass HU (1998) Transports between Oderhaff and Pomeranian bight — a simple barotropic box model (1998). *Dtsch Hydrogr Z* 50:371–383. <https://doi.org/10.1007/BF02764231>
- Osadczyk A, Wawrzyniak-Wydrowska B (1998) Sediments in the Szczecin Lagoon: Selected elements and macrozoobenthos. *Greifswalder Geographische Arbeiten* 16:169–193. [https://balticeucc.databases.eucc-d.de/files/documents/00000164\\_09\\_Sediments\\_in\\_the\\_Szczecin\\_Lagoon\\_fig\\_tab.pdf](https://balticeucc.databases.eucc-d.de/files/documents/00000164_09_Sediments_in_the_Szczecin_Lagoon_fig_tab.pdf). Accessed 14 May 2022
- Osadczyk A, Musielak S, Borówka R (2007) Why should the Odra River mouth area not be regarded as an estuary? A geologist's point of view. *Oceanol Hydrobiol Stud* 36(2):87–99. <https://doi.org/10.2478/v10009-007-0011-8>
- Pastuszak M, Witek Z, Nagel K, Wielgat M, Grelowski A (2005) Role of the Oder estuary (southern Baltic) in transformation of the riverine nutrient loads. *J Mar Syst* 57(1–2):30–54. <https://doi.org/10.1016/j.jmarsys.2005.04.005>
- Pein JU, Stanev EV, Zhang YJ (2014) The tidal asymmetries and residual flows in Ems Estuary. *Ocean Dyn* 64:1719–1741. 10.1007
- Pein J, Eisele A, Sanders T, Daewel U, Stanev EV, Van Beusekom JE, Staneva J, Schrum C (2021a) Seasonal stratification and biogeochemical turnover in the freshwater reach of a partially mixed dredged estuary. *Front Mar Sci* 8:623714. <https://doi.org/10.3389/fmars.2021.623714>
- Pein J, Staneva J, Daewel U, Schrum C (2021b) Channel curvature improves water quality and nutrient filtering in an artificially deepened mesotidal idealized estuary. *Cont Shelf Res* 231:104582. <https://doi.org/10.1016/j.csr.2021.104582>
- Pinto L, Fortunato AB, Zhang Y, Oliveira A, Sancho FEP (2012) Development and validation of a three-dimensional morphodynamic modelling system for non-cohesive sediments. *Ocean Modell* 57:1–14. <https://doi.org/10.1016/j.ocemod.2012.08.005>. Get rights and content
- Radziejewska T, Schernewski G (2008) The Szczecin (Oder-) Lagoon. In: Schiewer U (eds) *Ecology of Baltic Coastal Waters. Ecological Studies*, vol 197. Springer, Berlin, Heidelberg. [https://doi.org/10.1007/978-3-540-73524-3\\_5](https://doi.org/10.1007/978-3-540-73524-3_5)
- Schernewski G, Neumann T, Opitz D, Venohr M (2011) Long-term eutrophication history and ecosystem changes in a large Baltic river basin–estuarine system. *Transit Waters Bull* 5:21–49. <https://doi.org/10.1285/i1825229Xv5n2p21>
- Schernewski G, Stybel N, Neumann T (2012) Zebra Mussel Farming in the Szczecin (Oder) Lagoon: Water-Quality Objectives and Cost-Effectiveness. *Ecol Soc* 17(2). <http://www.jstor.org/stable/26269031>. Accessed 14 May 2022
- Schernewski G, Friedland R, Paysen S, Bucas M, Dahlke S, von Weber M (2023) Macrophytes and water quality in a large Baltic lagoon:

- relevance, development and restoration perspectives. *Front Mar Sci* 10:1049181. <https://doi.org/10.3389/fmars.2023.1049181>
- Schiewer U, Gerald S (2004) Self-purification capacity and management of Baltic coastal ecosystems. *J Coast Conserv* 10:25–32. [https://doi.org/10.1652/1400-0350\(2004\)010\[0025:SCAMOB\]2.0.CO;2](https://doi.org/10.1652/1400-0350(2004)010[0025:SCAMOB]2.0.CO;2)
- Schrum C, Alekseeva I, John MS (2006) Development of a coupled physical–biological ecosystem model ECOSMO: part I: model description and validation for the North Sea. *J Mar Syst* 61(1–2):79–99. <https://doi.org/10.1016/j.jmarsys.2006.01.005>
- Shen J, Haas L (2004) Calculating age and residence time in the tidal York River using three-dimensional model experiments. *Estuar Coast Shelf Sci* 61(3):449–461. <https://doi.org/10.1016/j.ecss.2004.06.010>
- Siegel H, Matthäus W, Bruhn R et al (1998) The exceptional Oder flood in summer 1997 — distribution patterns of the oder discharge in the Pomeranian Bight. *Deutsche Hydrographische Zeitschrift* 50:145–167. <https://doi.org/10.1007/BF02764484>
- Simpson JH (1981) The shelf-sea fronts: implications of their existence and behaviour. *Philos Trans R Soc Lond A* 302(1472):531–546. <https://doi.org/10.1098/rsta.1981.0181>
- Stanev EV, Jacob B, Pein J (2019) German Bight estuaries: An inter-comparison on the basis of numerical modeling. *Cont Shelf Res* 174:48–65
- Stokowski M, Schneider B, Rehder G, Kuliński K (2020) The characteristics of the CO<sub>2</sub> system of the Oder River estuary (Baltic Sea). *J Mar Syst* 211:103418. <https://doi.org/10.1016/j.jmarsys.2020.103418>
- Taylor KE (2001) Summarizing multiple aspects of model performance in a single diagram. *J Geophys Res Atmos* 106(D7):7183–7192. <https://doi.org/10.1029/2000JD900719>
- Voss M, Asmala E, Bartl I et al (2021) Origin and fate of dissolved organic matter in four shallow Baltic Sea estuaries. *Biogeochemistry* 154:385–403. <https://doi.org/10.1007/s10533-020-00703-5#>
- Wang Z, Chai F, Dugdale R et al (2020) The interannual variabilities of chlorophyll and nutrients in San Francisco Bay: a modeling study. *Ocean Dyn* 70:1169–1186. <https://doi.org/10.1007/s10236-020-01386-0>
- Ye F, Zhang YJ, Wang HV, Friedrichs MA, Irby ID, Alteljevich E, ... Du J (2018) A 3D unstructured-grid model for Chesapeake Bay: Importance of bathymetry. *Ocean Modell* 127:16–39. <https://doi.org/10.1016/j.ocemod.2018.05.002>
- Yumruktepe VÇ, Samuelsen A, Daewel U (2022) ECOSMO II (CHL): a marine biogeochemical model for the North Atlantic and the Arctic. *Geosci Model Dev* 15(9):3901–3921. <https://doi.org/10.5194/gmd-15-3901-2022>
- Zhang YJ, Ye F, Stanev EV, Grashorn S (2016) Seamless cross-scale modeling with SCHISM. *Ocean Model* 102:64–81. <https://doi.org/10.1016/j.ocemod.2016.05.002>